

Characteristics of Co/Cr Codoped Zinc Oxide[†]

REZQ N. ALJAWFI and S. MOLLAH*

Department of Physics, Aligarh Muslim University, Aligarh-202 002, India

*Corresponding author: E-mail: smollah@rediffmail.com

AJC-10349

In the present paper, we report the optical and magnetic properties of $Zn_{0.97}Co_{0.03}O$ and $Zn_{0.94}Cr_{0.03}Co_{0.03}O$, nanocrystalline powder diluted magnetic semiconductor, prepared by the sol-gel method. XRD patterns of the sample was indexed as hexagonal wurzite structure, the size of particles are 19 nm and 15 nm, respectively. UV-VIS optical absorption spectra results show that the band gap energy of the oxide semiconductor ZnO decrease with incorporation of Co and Cr in the ZnO lattice structure. Magnetic measurements performed by SQUID magnetometer reveals the presence of room temperature ferromagnetism.

Key Words: DMS, XRD, Optical properties, UV-VIS, FTIR, Magnetic properties, PACS: 61.05.cp, 78.20.Ci, 75.50.Tt.

INTRODUCTION

Transition metal doped ZnO based diluted magnetic semiconductors (DMS) systems are being extensively studied for various reasons. These are found to be the potential candidates for the application of spin polarized current in the field of spintronics¹. These systems also present many challenges to the understanding of the nature of their complex magnetism. The key requirement in the development of such systems is the efficient injection, transfer and detection of spin-polarized currents at or above room temperature. However, due to the well-known problem of lattice mismatch at metal-semiconductor interfaces, there is still hindrance in effective spin injection². Much interest is now concentrated on the development of ferromagnetic semiconductors at room temperature³. One approach to magnetize these semiconductors is light doping of magnetic ions into the host materials. Therefore, a non-magnetic semiconductor (like ZnO, TiO₂, InO₂, SnO₂) is doped with transition metal ion(s) (such as Co, Cr, Mn, Fe, Ni or V) to achieve magnetism^{3,4}. It is further observed that the 3d transition metal impurity should be of only few per cent of the cations, *i.e.* it must be very dilute in the non-magnetic matrix leading the term diluted magnetic semiconductor⁵. Zinc oxide diluted magnetic semiconductors has attracted a great deal of attention due to theoretical prediction of the possibility of ferromagnetic ordering above room temperature in transition metal doped ZnO, where ZnO has a wide band gap energy (3.37 eV) and high excitation

binding energy (60 MeV)^{3,6}. There are many reports on the ferromagnetism (FM) of transition metal doped ZnO, but no consensus has been reached about the coupling mechanism or even the origin of magnetic moments⁷. The origin of FM in diluted magnetic semiconductor materials is not understood completely. There are still some reports showing no sign of FM or suggesting the presence of secondary phase as the origin of FM in diluted magnetic semiconductor⁸. Number of studies indicates that the FM in transition metal-doped ZnO may come from the precipitation of magnetic clusters or from the secondary magnetic phases⁹. Almost all these reports create doubt about whether the transition metal doping or defects are responsible for the observed magnetism in ZnO¹⁰. Therefore, there is a strong incentive to develop a new diluted magnetic semiconductor material that exhibits the desired properties. Synthesis methods adopted for the preparation of diluted magnetic semiconductor materials also have effect on their magnetization properties. In this report, we study the effect of Cr, Co on the optical and magnetic properties of ZnO semiconductor, where ZnO is diamagnetic and Co doped ZnO is n type semiconductor. The exchange interactions between the band electrons and the localized *d* electrons of the Co²⁺ that are substituting Zn²⁺ play important role in the magnetic properties. Also the defect such as cluster of Co metal is one of the possibility as the source of magnetic properties. The samples show the ferromagnetic properties at room temperature.

[†]Presented to the National Conference on Recent Advances in Condensed Matter Physics, Aligarh Muslim University, Aligarh, India (2011).

EXPERIMENTAL

The samples were synthesized by the sol-gel method. Analytical reagents (AR) grade zinc nitrate [$\text{Zn}(\text{NO}_3)_2 \cdot 6\text{H}_2\text{O}$], chromium nitrate [$\text{Cr}(\text{NO}_3)_3 \cdot 9\text{H}_2\text{O}$], cobalt nitrate [$\text{Co}(\text{NO}_3)_2 \cdot 6\text{H}_2\text{O}$] and citric acid [$\text{C}_6\text{H}_8\text{O}_7 \cdot \text{H}_2\text{O}$] were used as the raw materials without any special treatment. These were taken with desired stoichiometric ratio. Nitrates were dissolved in distilled water to get homogeneous solution by using magnetic stirrer at 70 °C. Citric acid had been dissolved separately in distilled water for 0.5 h and then added to the nitrate solution. Slowly, molarity ratio of nitrate to citric acid was 1:1. The solution was continuously stirred at 70 °C until it was converted into gel form. Then it was heated at 130 °C for 12 h. The product was grinded for 0.5 h to get amorphous oxide powder of samples. Final annealing of all the samples was done in furnace at 450 °C for a duration of 12 h in air followed by grinding to obtain the required sample.

X-ray diffraction (XRD) pattern of the samples was obtained at room temperature, with step of 0.02°, using Bruker D8 ADVANCE X-ray diffractometer with $\text{CuK}\alpha$ radiation ($\lambda = 1.54178 \text{ \AA}$) in the range of $20^\circ \leq 2\theta \leq 100^\circ$ at 40 kV. FTIR spectra was taken on Perkin-Elmer BX2 FTIR spectrometer using KBr pellets as medium, at room temperature. The optical absorbance spectra were recorded using a UV-visible double beam Perkin-Elmer, LAMDA 35 spectrophotometer, at room temperature in the wavelength range 250–800 nm. Magnetization properties of the samples have been studied by utilizing superconducting quantum interference device (SQUID), system (MPMS-XL) produced by QUANTUM DESIGN.

RESULTS AND DISCUSSION

X-ray diffraction studies: Structure of $\text{Zn}_{0.97}\text{Co}_{0.03}\text{O}$ and $\text{Zn}_{0.94}\text{Cr}_{0.03}\text{Co}_{0.03}\text{O}$ samples have been determined by XRD at room temperature (Fig. 1). Diffraction peaks are found to be in good agreement with the standard peak positions of ZnO (JCPDS card no. 36-1451). XRD pattern exhibit single phase. No observed secondary phase in the samples within the sensitivity of XRD technique, which confirms that the chemical reaction by sol gel method has been performed successfully and all starting organic precursors might have been completely decomposed. Lattice parameter calculation and indexing of the diffraction peaks of the samples are done by using the powder X-ray diffraction refinement program and found to be in good agreement with the reported values. The samples possess the hexagonal wurtzite structure with space group $p63mc$. The values of lattice parameters 'a' and 'c' are found to be 3.248, 5.211 for $\text{Zn}_{0.97}\text{Co}_{0.03}\text{O}$ and 3.247, 5.208 for $\text{Zn}_{0.94}\text{Cr}_{0.03}\text{Co}_{0.03}\text{O}$, respectively, that indicates to the decrease in the lattice para-meter with adding Cr that attributes to that the ionic radii of Co/Cr which are smaller than of Zn. The size of particles has been calculated using Debye-Scherrer's formula:

$$D = 0.9\lambda/\beta \cos\theta \quad (1)$$

where D is the diameter of the particles, λ is the wavelength of X-ray (1.54178 Å), θ is the Bragg angle at the full width and of half maxima (FWHM) on the highest peak of plane (101) at $\sim 2\theta = 36.27^\circ$. The size of particle is found to be 15–19 nm.

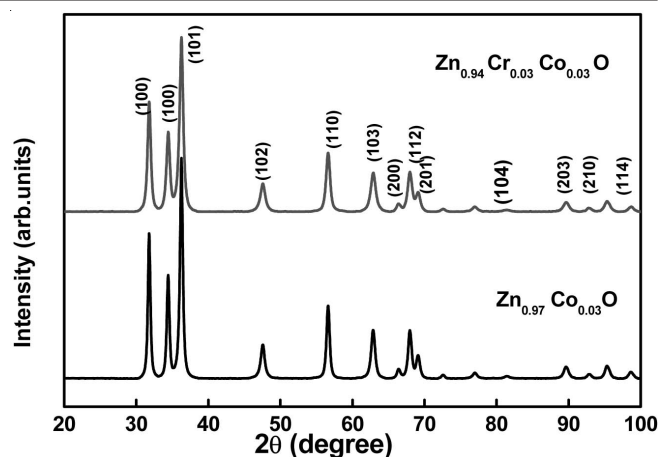


Fig. 1. X-ray diffraction pattern of $\text{Zn}_{0.97}\text{Co}_{0.03}\text{O}$ and $\text{Zn}_{0.94}\text{Cr}_{0.03}\text{Co}_{0.03}\text{O}$ samples

Optical properties: To make sure that Co^{2+} , Cr^{3+} have been doped into the Zn^{2+} lattice, room-temperature UV-VIS optical absorption spectra have been recorded as shown in Fig. 2(a). Absorption peaks appear at ~ 360 and ~ 274 nm. The corresponding band gap energies are ~ 3.41 and ~ 4.5 eV, respectively. The direct band gap energy (E_g) is calculated using the Tauc equation:

$$(\alpha h\nu)^2 = B (h\nu - E_g)^n \quad (2)$$

where $h\nu$ = photon energy, α = absorption coefficient, E_g = band gap energy, B = constant and n = exponent which takes values of 1/2 for direct and 2 for indirect electronic transition in k-space. Fitting the data with eqn. 2 for different n values, $n = 1/2$ was found to give the best fit. Fig. 2(b) demonstrates the $(\alpha h\nu)^2$ plotted as a function of hc/λ . Value of direct band gap energy has been found by extrapolating the straight line down to $(\alpha h\nu)^2 = 0$. Direct band gap energy for all the samples is ~ 3.03 . It is well known that the band gap energy (E_g) of pure ZnO is 3.3 eV at 300 K and absorption edge of $\text{Zn}_{0.97}\text{Co}_{0.03}\text{O}$ sample shifts towards lower energy ~ 3.03 eV. This decrease in band gap energy (red shift) is observed in other reports also which is the evidence that the Co^{2+} has got incorporated into the lattice structure of ZnO ¹¹. It is also in good agreement with the reported value (3.00 eV) for $\text{Zn}_{0.9}\text{Co}_{0.1}\text{O}$ ^{12,13}. For sample $\text{Zn}_{0.94}\text{Cr}_{0.03}\text{Co}_{0.03}\text{O}$, the band gap energy increases with adding Cr to 3.08 eV. This is interpreted as mainly due to the $sp-d$ exchange interactions between the band electrons and the localized d electrons of the Co^{2+} ions that are substituting Zn^{2+} ions¹². The exchange interactions between $s-d$ and $p-d$ orbitals give rise to a negative and a positive correction to the conduction-band and valence-band edges, respectively, resulting to a decrease in band gap^{12,13}. It is also in accordance with the results of Cd doped ZnO where the band gap of $\text{Zn}_{1-x}\text{Cd}_x\text{O}$ comes out to be to 3.00 eV instead of standard value 3.3 eV for ZnO, Similar result is also found for V doped ZnO ¹⁴. It is observed that the decrease in the size of particles leads to decrease in the band gap energy that may be due to the size quantization effect, which lead to enhanced band bending of crystal at grain surface.

FTIR spectrum studies: The formation of ZnO wurtzite structure in the nanocrystalline sample is further supported by the FTIR spectra (Fig. 3). The absorption band at *ca.* 3400

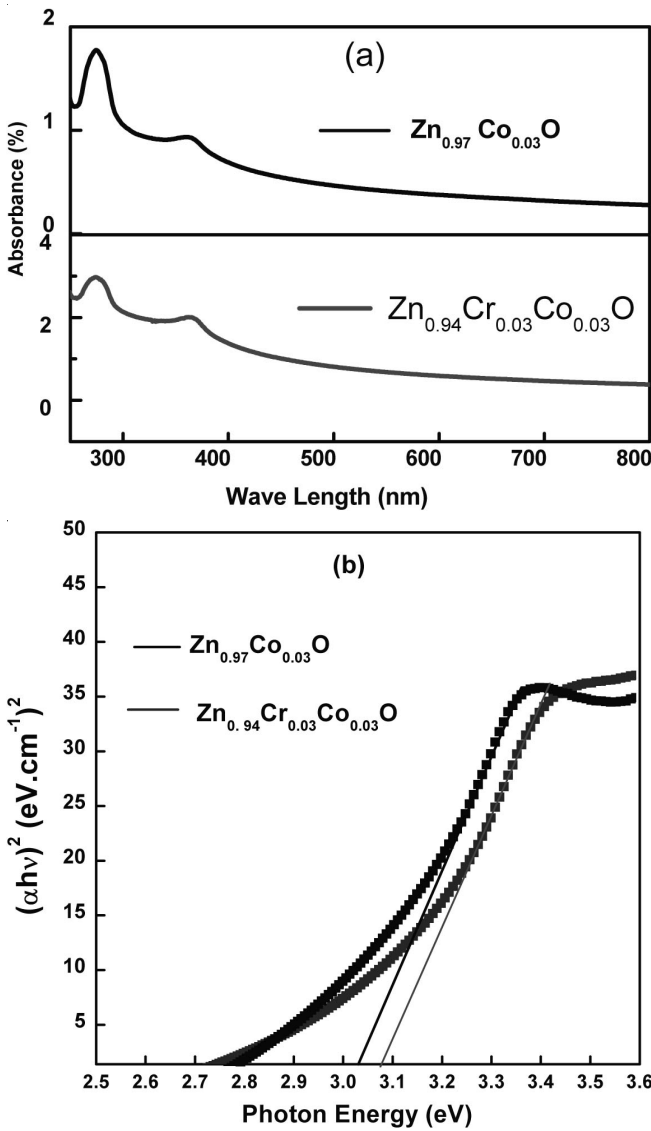


Fig. 2. (a) Room temperature optical absorption spectra and (b) $(\alpha E)^2$ vs. energy plot for $Zn_{0.97}Co_{0.03}O$ and $Zn_{0.94}Cr_{0.03}Co_{0.03}O$ samples

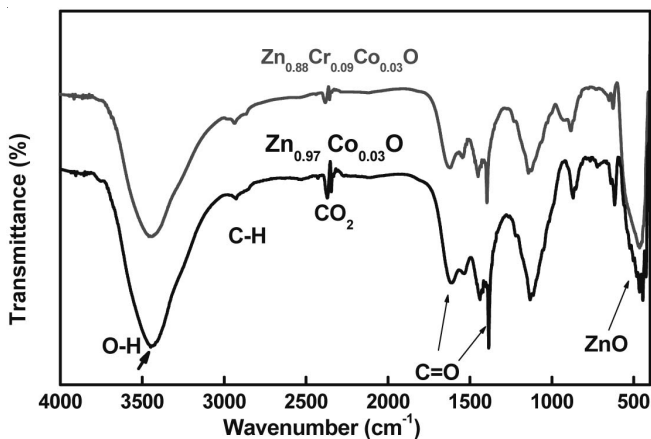


Fig. 3. FTIR spectra of $Zn_{0.97}Co_{0.03}O$ and $Zn_{0.94}Cr_{0.03}Co_{0.03}O$ samples

cm^{-1} represents the stretching vibration of O-H mode for hydroxide group or for interlayer water molecule H_2O (free or bonded)¹⁵. Small band appears at ~ 2900 cm^{-1} which is featured to the C-H bond of organic compounds. The peaks at ~ 2340 cm^{-1} may be due to the absorption of CO_2 from the

atmosphere¹⁵. Absorption bands at *ca.* 1600 and 1380 cm^{-1} are, respectively, the symmetric and asymmetric C=O stretching modes. The absorption band in the range of 1500-1000 cm^{-1} represents the vibration of ions in the crystal lattice. The peaks at 450 and 480 cm^{-1} are due to stretching mode of ZnO¹². Absorption bands observed in the ranges from 645 to 600 cm^{-1} and from 462 to 457 cm^{-1} are attributed to the stretching modes of ZnO.

Magnetization: The magnetization of $Zn_{0.97}Co_{0.03}O$ and $Zn_{0.94}Cr_{0.03}Co_{0.03}O$ samples have been studied by SQUID magnetometer. Magnetization (M) plotted as a function of the applied magnetic field (H) at room temperature. Fig. 4 shows clear M-H hysteresis loops that indicate the presence of room temperature ferromagnetism (RTFM). The hysteresis loop of $Zn_{0.97}Co_{0.03}O$ exhibits ferromagnetic hysteresis curve with the coercive field $H_C = -68.63$ Oe and the remanent magnetization $M_R = 6.56 \times 10^{-4}$ emu/g and saturated magnetization $M_S = 6 \times 10^{-3}$ emu/g. With addition of Cr in the sample ($Zn_{0.94}Cr_{0.03}Co_{0.03}O$), the coercive field becomes $H_C = 84$ Oe, the remanent magnetization $M_R = 8.77 \times 10^{-4}$ emu/g and saturated magnetization $M_S = 7.1 \times 10^{-3}$ emu/g. The origin of ferromagnetism may be secondary phases such as CoO or Co-cluster domain. But CoO is antiferromagnetic with small positive susceptibility having $T_N \sim 293$ K^{16,17} and the Co-metal exhibits ferromagnetism with T_N of ~ 1400 K¹⁸. However the XRD data do not support the

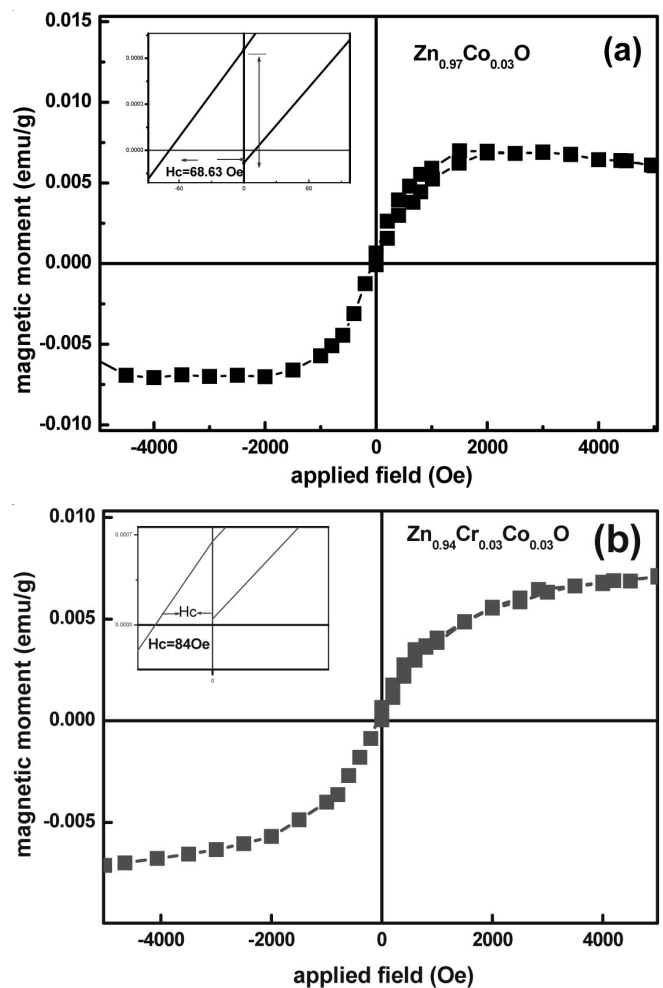


Fig. 4. M-H curves at 300 K (a) $Zn_{0.97}Co_{0.03}O$ and (b) $Zn_{0.94}Cr_{0.03}Co_{0.03}O$ samples. The insets show the H_C and M_R for the samples

presence of Co-metal or CoO in the sample within the sensitivity of XRD technique, Therefore, the possibility of ferromagnetism due to Co-cluster or CoO can be ruled out^{16,17}, the RTFM can be explained by Ruderman-Kittel-Kasuya-Yosida (RKKY) theory^{18,19}. According to this theory, the magnetization is due to exchange interaction between local spin-polarized electrons (such as Co²⁺) and conduction electrons. The interaction leads to the spin-polarization of conduction electrons. Subsequently, the spin-polarized conduction electrons perform an exchange interaction with local spin-polarized electrons of other Co²⁺ ions. Consequently, the long-range exchange interactions lead almost all the Co²⁺ ions to have same spin direction. The conduction electrons act as media for the interaction among the Co²⁺ ions. By adding Cr in the sample (Zn_{0.94}Cr_{0.03}Co_{0.03}O) the magnetization increases and may be explained by the increase of the current carriers (hole or electrons) in the valance band. The induced FM in Co doped ZnO has already been observed by other groups⁸. That attributes to the FM behaviour in nanocrystals simply to magnetic dipoles located at the surface of nanocrystals, which interact with their nearest neighbours inside the crystal. Consequently, the interchange energy in these magnetic dipoles make other neighboring dipoles oriented in the same direction. In nanocrystals, surface-to-volume ratio increases. Hence, the population of magnetic dipoles oriented in the same direction will increase at the surface. Thus, the sum of the total amount of dipoles oriented along the same direction will increase. In short, the crystal surface will be usually more magnetically oriented²⁰.

Conclusion

Nanocrystalline powders of diluted magnetic semiconductor Zn_{0.97}Co_{0.03}O and Zn_{0.94}Cr_{0.03}Co_{0.03}O were successfully synthesized by sol-gel method. The annealing temperature was 450 °C. XRD pattern show single phase for the samples and possesses the hexagonal wurtzite structure. The size of particles decrease in Zn_{0.94}Cr_{0.03}Co_{0.03}O compared to that of 19 nm for the sample Zn_{0.97}Co_{0.03}O. Optical measurements using UV-visible spectrometer shows the evidence of the incorporation

of Co²⁺ and Cr³⁺ ions into the nonmagnetic host lattice of ZnO without any modification in the structure. The origin of ferromagnetism in these diluted magnetic semiconductor nanomaterial is due to the interaction and polarization of the localized electrons and the current carriers (electrons or holes). The defect may play an important role for inducing the uncoupled electron spin.

REFERENCES

1. D.D. Awschalom and M.E. Flatte, *Nat. Mater.*, **31**, 53 (2007).
2. G. Schmidt, D. Ferrand, L.W. Molenkamp and B. van Wees, *J. Phys. Rev. B*, **62**, 4790 (2000).
3. Y. Liu, J. Yang, Q. Guan, L. Yang and Y. Zhang, *J. Alloys Compd.*, **486**, 835 (2009).
4. S.J. Pearton, W.H. Heo, M. L'vill, D.P. Norton and T. Steiner, *Semicond. Sci. Technol.*, **19**, 59 (2004).
5. T.P.J. Han, M. Villegas, M. Peiteado, A.C. Caballero, F. Rodriguez and F. Jaque, *J. Chem. Phys. Lett.*, **488**, 173 (2010).
6. Y.B. Zhang, M.H.N. Assadi and S. Li, *J. Phys. Condens. Matter.*, **23**, 066004 (2011).
7. S.S. Li and Y.M. Hu, *J. Physics: Conference Series*, **266**, 012018 (2011).
8. Y. Liu, J. Yang, Q. Guan, L. Yang, H. Liu, Z. Wang, Y. Wang, D. Wang, Z.Q. Chen, D.D. Wang, N. Qi, J. Gong, C.Y. Cao and Z. Tang, *J. Appl. Surface Sci.*, **256**, 3559 (2010).
9. S. Ramachandran, A. Tiwari and J. Narayan, *Appl. Phys. Lett.*, **84**, 5255 (2004).
10. M. Snure, D. Kumar and A. Tiwari, *J. ProQuest Sci.*, **90**, 79 (2001).
11. Y. Xu, T. Yongjun, Y. Tang, C. Li, G. Cao, W. Ren, H. Xu and Z. Ren, *J. Alloys Compd.*, **481**, 837 (2009).
12. S. Maensiri, P. Laokul and S. Phokha, *J. Magn. Magn. Mater.*, **305**, 381 (2006).
13. M. Bouloudenine, N. Viart, S. Colis, J. Kortus and A. Dinia, *Chem. Phys. Lett.*, **397**, 73 (2004).
14. R. Elilarassi and G. Chandrasekaran, *J. Mater. Chem. Phys.*, **123**, 450 (2010).
15. S. Maensiri, P. Laokul and J. Klinkaewnarong, *J. Magn. Magn. Mater.*, **302**, 448 (2006).
16. C.J. Cong, J.H. Hong and K.L. Zhang, *Mater. Chem. Phys.*, **113**, 435 (2009).
17. K. Ueda, H. Tabata and T. Kawai, *Appl. Phys. Lett.*, **79**, 988 (2001).
18. M.A. Ruderman and C. Kittel, *Phys. Rev.*, **96**, 99 (1954).
19. K. Yosida, *Phys. Rev.*, **106**, 893 (1957).
20. P.K. Sharma, R.K. Dutta and A.C. Pandey, *J. Magn. Magn. Mater.*, **321**, 3457 (2009).